IIE Transactions (2003) **35**, 329–342

0740-817X/03 $12.00 + .00
DOI: 10.1080/07408170390184053

Tolerance allocation for compliant beam structure assemblies

B.W. SHIU[1], D.W. APLEY[2], D. CEGLAREK[3,*] and J. SHI[4]

[1]*Department of Mechanical Engineering, The Hong Kong Polytechnic University, Hung Hom, Kowloon, Hong Kong*
E-mail: mmbshiu@polyu.edu.hk
[2]*Department of Industrial Engineering, Texas A & M University, College Station, TX 77843, USA*
E-mail: apley@tamu.edu
[3]*Department of Industrial Engineering, University of Wisconsin, Madison, Madison, WI 53706, USA*
E-mail: darek@engr.wisc.edu
[4]*Department of Industrial and Operations Engineering, University of Michigan, Ann Arbor, MI 48109, USA*
E-mail: shihang@umich.edu

Received June 1999 and accepted June 2002

This paper presents a tolerance allocation methodology for compliant beam structures in automotive and aerospace assembly processes. The compliant beam structure model of the product does not require detailed knowledge of product geometry and thus can be applied during the early design phase to develop cost-effective product specifications. The proposed method minimizes manufacturing costs associated with tolerances of product functional requirements (key product characteristics, KPCs) under the constraint(s) of satisfying process requirements (key control characteristics, KCCs). Misalignment and fabrication error of compliant parts, two critical causes of product dimensional variation, are discussed and considered in the model. The proposed methodology is developed for stochastic and deterministic interpretations of optimally allocated manufacturing tolerances. An optimization procedure for the proposed tolerance allocation method is developed using projection theory to considerably simplify the solution. The non-linear constraints, that ellipsoid defined by $\boldsymbol{\tau}$ (stochastic case) or rectangle defined by $\mathbf{T_x}$ (deterministic case) lie within the KCC region, are transformed into a set of constraints that are linear in σ (or T_x)-coordinates. Experimental results verify the proposed tolerance allocation method.

Nomenclature

- $\{\boldsymbol{P}\}$ = total structural force applied to the whole structure;
- $[\boldsymbol{K}]$ = total stiffness matrix of the whole structure;
- $\{\boldsymbol{\Delta}\}$ = displacement of the whole structure under the influence of $\{\mathbf{P}\}$;
- $\{\boldsymbol{P}\}_i$ = total structural forces applied to the structure at node i;
- $\{\boldsymbol{\Delta}\}_i$ = structure displacement due to structural forces at node i;
- $[\boldsymbol{K}]_{ii}$ = direct structure stiffness matrix in global coordinate;
- $[\boldsymbol{k}]_{ij}$ = cross stiffness matrix, relating to forces at the i end to the displacement of j end;
- $[\boldsymbol{k}]_{ij}^{j}$ = direct stiffness matrix, relating to forces and displacement at the i end;
- $[\boldsymbol{K}]_{ij}$ = cross structure stiffness matrix in global coordinate;
- $[\boldsymbol{\beta}]_{ij}$ = compatibility matrix (transformation of member axis to global axis);
- $\{\boldsymbol{\delta}_s\}_{ij}$ = member ij displacement caused by the fabrication error;
- $\delta_x, \delta_y, \delta_z$ = magnitude of translation fabrication error in x, y, z direction respectively;
- $\theta_x, \theta_y, \theta_z$ = magnitude of rotation fabrication error in x, y, z direction respectively;
- $x_i, \mathbf{x}$ = variables and vector of Key Control Characteristics (KCCs);
- $z_i, \mathbf{z}$ = variable and vector for Key Product Characteristics (KPCs);
- $T_{x_i}, \mathbf{T_x}$ = constraint elements and vector for tolerance allocation;
- $T_{z_i}, \mathbf{T_z}$ = constraint elements and vector for tolerance analysis;
- $\mathbf{C}$ = KCC and KPC relationship matrix for tolerance allocation;
- $\mathbf{c}_i$ = the vector of $\mathbf{C}$ matrix in tolerance allocation KCC and KPC relationship matrix;
- A_i = the ith cost function coefficient assignment for the ith variable;
- $\boldsymbol{y}_i$ = normalized constraint vector;

* Corresponding author

- S_i = linear variety of the constraints defined by $\boldsymbol{y}_i$;
- $\boldsymbol{v}_i$ = vector in S_i with minimum norm;
- $\bar{\boldsymbol{y}}_i$ = modified constraints constant vector;
- σ_i = sigma designation of the optimization variables;
- $\boldsymbol{\Sigma}$ = diagonal vector of inverse of major axis dimension of ellipsoid;
- K = a variable obtained from χ^2 distribution with certain confidence level;
- α = confidence level of the probability of a point within the ellipsoid.

1. Introduction

Manufacturing companies in various industries, including automotive and aerospace, are generally interested in predicting the effects of part and tooling variation on final product quality during the design stage (Juster, 1992; Liu *et al.*, 1995). Dimensional variation of the final product caused by part variation and assembly tooling dimensional discrepancies decreases product functionality such as automobile performance (e.g., wheel misalignment, squeaks and rattles, or vibration) and increases warranty costs (e.g., problems related to wind noise, door closing efforts or panel closure alignment). Problems caused by dimensional variation include rework, quality rejects and resulting engineering changes.

Whenever a component is manufactured, there are small variations in its size and shape from the desired design nominal. These variations are an inevitable fact of any manufacturing process. In general, dimensional variation is caused by: (i) part-to-part interference; (ii) lack of stability in part location; and (iii) part variation. Interference is dependent on the types of joints between various parts and part fabrication error, whereas locating instability (part misalignment) is dependent on the types and positions of locators in the assembly stations. Interference and misalignment were identified in the aerospace and automotive industries as the two most frequent causes of engineering changes (Shalon *et al.*, 1992; Ceglarek and Shi, 1995). A third cause of dimensional variation, part variation, is due to fabrication error occurring during the part manufacturing process (e.g., stamping or machining).

To account for these sources of dimensional variation, the designer specifies allowable limits, or tolerances, on the dimensions. For example, when knowledge of actual assembly process behavior (such as welding induced internal stress or part misalignment in fixtures) and/or component characteristics (such as flexibility of sheet metal or fabrication error) is limited, tolerances ensure acceptable functional requirements, given variations in assembly process behavior and component characteristics. Thus, tolerances accommodate the uncertainty that is inherent in engineering practice and manufacturing processes. Tolerances that are set too wide can result in poor quality, while overly-tight tolerances generally result in increased manufacturing costs.

Product quality is generally characterized by a group of features that affect the designed functionality and the level of customer satisfaction. In the automotive industry, this group of critical features is referred to as Key Product Characteristics (KPCs), an example of which is dimension z_1 in Fig. 1. The fixture locators or part joint(s) position errors are the dimensional control characteristics for product positioning, and thus are the determining factors in achieving the required dimensional accuracy of the KPCs. These are referred to as Key Control Characteristics (KCCs), examples of which are x_1, x_2, and x_3 in Fig. 1. The impact of KCC variation on KPC dimensional accuracy depends on the process configuration, which includes the geometry/layout of locating fixtures and part-to-part joints/mating features. An intuitive decomposition of product and process into key characteristics is discussed in Ceglarek *et al.* (1994), Ceglarek and Shi, (1996), whereas Thornton (1999) proposed a more mathematical framework.

Referring to Fig. 1, the manufacturing process must maintain sufficiently small variations in the dimensional lengths of x_1, x_2, and x_3 in order to produce sufficiently small variations in final assembly dimension z_1.

The goal of tolerance allocation is to optimally allocate tolerances to the KCCs, subject to constraints on the tolerances of the KPCs. Optimality is usually understood to mean some measure of manufacturing cost (which increases with tighter KCC tolerances) subject to product requirements (which defines the KPCs constraints) (Lee and Woo, 1990).

Increasingly, emphasis is being placed on integrating manufacturing considerations from product tolerance specification(s) (Juster 1992; Liu *et al.*, 1996). This is of great importance because product accuracy cannot be disassociated from the manufacturing process. Difficulties in integrating manufacturing process information with

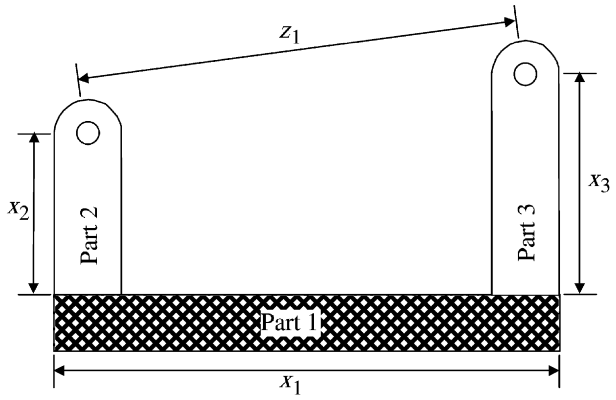

Fig. 1. An example of the KPC and KCC relationship.

product characteristics have been observed by many researchers (e.g., Hillyard and Braid, 1978; Faux, 1986; Etesami, 1993; Roy *et al*., 1991; Zhang, 1997; Hong and Chang, 2002; Chase *et al*., 1990; Kumar and Raman, 1992; Nigam and Turner, 1995; Liu *et al*., 1996; Ceglarek and Shi, 1997; Voelcker, 1998; Choudhuri and DeMeter, 1999). The traditional ANSI tolerancing methods are no longer applied in sheet metal assembly or, in general, in compliant structure assemblies (Takezawa, 1980; Liu *et al*., 1996). Liu *et al*. (1996) developed a method of tolerance analysis in compliant sheet metal assembly using one-dimensional linear mechanics that take into account the assembly behavior of component/part characteristics. Limitations of three-dimensional assembly tolerance analysis, such as the lack of appropriate statistical and assembly interaction models, are discussed in Scott and Gabriele (1989) and Chase and Parkinson (1991). However, these works have not investigated a three-dimensional compliant structure assembly incorporating the product/design dimensional and functional requirements.

The most common approaches to tolerance allocation are based on recursive Monte Carlo simulation, non-linear programming, or first order Taylor series approximations (Lehtihet and Dindelli, 1989; Eggert and Mayne, 1990; Parkinson *et al*., 1990; Jastrzebski, 1991). Some of the shortcomings of the Monte Carlo simulation include intensive computational requirements and inaccurate results for small sample sizes (Nigam and Turner, 1995). The probabilistic tolerance optimization problem can be simplified to a deterministic non-linear programming problem (Parkinson, 1985; Anderson, 1990; Lee and Woo, 1990). The Taylor series approach (Lee and Woo, 1990) is an approximate method in which non-linear tolerance constraints are linearized. This results in a computationally expensive algorithm due to the recursive approach needed to find the optimal solution. In addition to the computational expense, these methods are somewhat difficult to implement.

Another main body of tolerance allocation research is based on cost optimization. The tolerance allocation problem is to systematically search for the combination of tolerances which results in the least overall manufacturing cost, while at the same time satisfying all dimensional requirements. Numerous researchers have proposed different search algorithms and different forms of explicit cost functions (Parkinson, 1984, 1985; Wu *et al*., 1988; Lee and Woo, 1990; Chase and Parkinson, 1991; Guilford and Turner, 1993). They are based mainly on estimated algebraic cost functions. A further refinement of cost tolerancing is based on association of cost with different manufacturing processes. Consideration is given to processes that can most economically produce each part dimension while satisfying tolerance of all parts (Bjorke, 1989; Lee and Woo, 1989; Ostwald and Blake, 1989; Chase *et al*., 1990).

There is no existing algorithm for tolerance allocation in three-dimensional compliant structure assemblies. In this paper, a tolerance allocation algorithm that is relatively straightforward to implement will be developed for this scenario. The proposed algorithm allows designers to specify and verify proper tolerances for compliant structure assemblies at the design stage. This method integrates characteristics of both the assembly process and the final product. Additionally, this method uses design requirements as constraints while minimizing manufacturing costs in order to maximize the allowable tolerances in each of the process characteristics or process control points.

2. Review of fabrication error in structure analysis

A beam-based model of an automotive body has been used to analyze the bending and torsional stiffness of the vehicle structure with high accuracy. These models (Chon *et al*., 1986) allow one to predict the distortion of the automotive body under external loading such as driving, cargo, and passenger loads. Recent dimensional control applications have used similar concepts (Ceglarek and Shi, 1997; Shiu *et al*., 1997; Rong *et al*., 2000; Rong *et al*., 2001). The use of a beam-based model for tolerancing of compliant assembly structures offers the following benefits:

1. Beam structures allow for the modeling of major product dimensional discrepancies caused by: (i) part-to-part interference; (ii) lack of part location stability (part misalignment during assembly); and (iii) part fabrication error variation;
2. Tolerancing must be considered early during the design phase in order to develop cost-effective product specifications (Narahari *et al*., 1999; Voelcker, 1998). However, existing approaches to allocate tolerances require detailed knowledge of the geometry of the assemblies and are applicable mostly during the advanced stages of design, leading to a less than optimal design process. During the design process of assemblies, both the assembly structure and associated tolerance information evolve continuously. Therefore, significant gains can be achieved by effectively using this information to influence the design of the assembly. It was shown in Ceglarek and Shi (1997), Shiu *et al*. (1997), and Rong *et al*. (2000) and Rong *et al*. (2001) that the beam-based model provides a simplified but effective representation of tolerancing information during the early stages of design that can be used to model dimensional discrepancies before detailed 3D CAD models are available. The development of the beam-model requires only limited information such as part stiffness (modeled via beams) and geometrical position of both ends, which is consistent with the

information that is used during the early stages of the design process. The detailed part geometries are typically not determined until the later stages of the design process and are based on the structural requirements from the early stages. Hence, the beam-based tolerancing approach is well-suited for use during the very early stages of design.

In structural analysis (West, 1993), member (beam or part) interactions can be viewed as self-straining. Fabrication error is defined as the self-straining phenomenon caused by the assembly of erroneous or misaligned components into a structure. Interaction occurs when a structure is subjected to internal strains and a resulting state of stress with no externally applied forces. An example is the interaction of assembly faults caused by dimensional errors in fixtured parts, in which a member or part of erroneous length or alignment is forced to fit during the assembly process. Such an assembly fault is characterized as statically indeterminate. The structure responds to the fabrication error by equalizing the internal stresses caused by the erroneous parts. The resulting internal stresses generate related self-equilibrating external reactions. The structure itself serves to inhibit the deformation and is "straining against itself."

These fabrication error concepts apply to automotive body assembly, as illustrated in Fig. 2. Part misalignment and fabrication errors are the major sources of variation and errors in the automotive assembly process. The induced structure forces from fabrication errors are used in the stiffness analysis. Assume members a-b, c-d, e-f, and g-h have fabrication errors as shown in Fig. 2. For example, node a of the a-b beam has a fabrication error of $\{\boldsymbol{\delta}_s\}_{ab} = [0(\delta_s)_2 0\ 0\ 0\ 0]^T_{ab}$ (i.e., dimensional error in y direction), the fabrication error of node b is $\{\boldsymbol{\delta}_s\}_{ba} = [0(\delta_s)_2(\delta_s)_3\ 0\ 0\ 0]^T_{ba}$ (i.e., dimensional errors in the y and z directions), and so on.

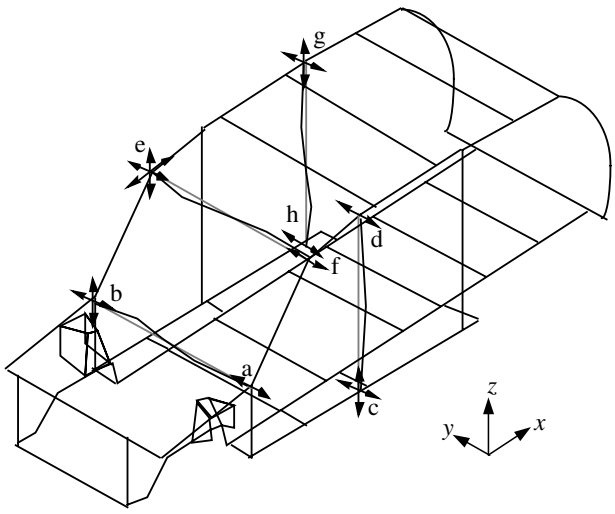

Fig. 2. The automotive body structure with fabrication error.

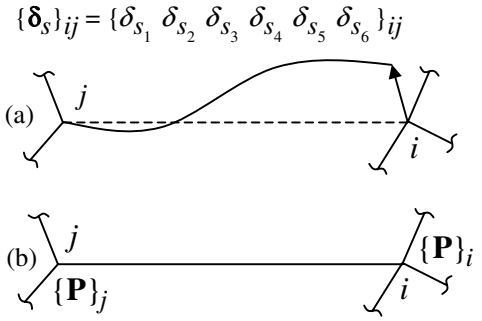

Fig. 3. Self-straining in structure analysis: (a) fabrication error of a single beam within a structure; and (b) forces required to correct the fabrication error.

Figure 3(a) shows a generic member ij with fabrication error denoted by the solid line, whereas, the nominal design is the dashed line. The fabrication error is represented by the vector $\{\boldsymbol{\delta}_s\}_{ij} = \{\delta_{s_1}\delta_{s_2}\delta_{s_3}\delta_{s_4}\delta_{s_5}\delta_{s_6}\}_{ij}$. If this displacement is restrained (i.e., if the displacement $-\{\boldsymbol{\delta}_s\}_{ij}$ is applied to correct the error), a set of fixed-end forces is imposed at joints i and j as shown in Fig. 3(b). If the structure analysis is limited to fabrication error, then the equivalent force $\{\boldsymbol{P}\}_i$ that is required to self-restrain the error is

$$\{\boldsymbol{P}\}_i = -\sum_j [\boldsymbol{\beta}]^T_{ij}(-[\boldsymbol{k}]^j_{ii}\{\boldsymbol{\delta}_s\}_{ij}) \tag{1}$$

where $[\boldsymbol{\beta}]^T_{ij}$ and $[\boldsymbol{k}]^j_{ii}$ are the compatibility matrix and cross stiffness matrix defined in West (1993).

Moreover, for an n-noded structure, the overall structural displacement for all nodes can be expressed as a function of the equivalent forces via

$$\begin{bmatrix} \{\boldsymbol{\Delta}\}_1 \\ \{\boldsymbol{\Delta}\}_2 \\ \{\boldsymbol{\Delta}\}_3 \\ \cdots \\ \{\boldsymbol{\Delta}\}_n \end{bmatrix} = \begin{bmatrix} [\boldsymbol{K}]_{11} & [\boldsymbol{K}]_{12} & [\boldsymbol{K}]_{13} & \cdots & [\boldsymbol{K}]_{1n} \\ [\boldsymbol{K}]_{21} & [\boldsymbol{K}]_{22} & [\boldsymbol{K}]_{23} & \cdots & [\boldsymbol{K}]_{2n} \\ [\boldsymbol{K}]_{31} & [\boldsymbol{K}]_{32} & [\boldsymbol{K}]_{33} & \cdots & [\boldsymbol{K}]_{3n} \\ \cdots & \cdots & \cdots & \cdots & \cdots \\ [\boldsymbol{K}]_{n1} & [\boldsymbol{K}]_{n2} & [\boldsymbol{K}]_{n3} & \cdots & [\boldsymbol{K}]_{nn} \end{bmatrix}^{-1} \begin{bmatrix} \{\boldsymbol{P}\}_1 \\ \{\boldsymbol{P}\}_2 \\ \{\boldsymbol{P}\}_3 \\ \cdots \\ \{\boldsymbol{P}\}_n \end{bmatrix}. \tag{2}$$

The significance of the preceding results is that Equations (1) and (2) can be combined to give

$$[\boldsymbol{\Delta}] = F(\boldsymbol{\delta}). \tag{3}$$

The vector $\boldsymbol{\Delta}$ represents the nodal displacements with $6n$ elements for an n-noded structure, the vector $\boldsymbol{\delta}$ represents the fabrication error of each individual part, and F represents the linear relationship obtained from a structure analysis formulation (West, 1993).

3. Linear/linearized model relating KPCs to KCCs

Consider the simple beam-based structure shown in Fig. 4. The solid beams represent the nominal dimensions

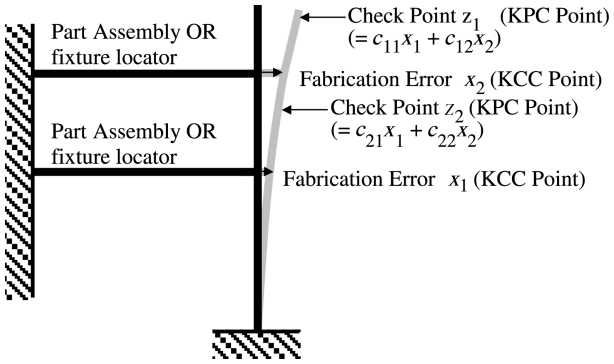

Fig. 4. Illustration of the linearity of a flexible assembly.

of the structure, and the shaded beams the actual dimensions. The structural stress caused by fabrication errors ($\boldsymbol{\delta}$ of Equation (3)) in the two horizontal components will influence the overall dimensional integrity ($\boldsymbol{\Delta}$ of Equation (3)) of the vertical beam. If the assembly process were perfect in both the tooling conditions and the dimensions of the detail parts, the resulting assembly would be the solid beam of Fig. 4. In practice, however, each of the two beams will contain fabrication errors inherited from the tooling errors, parts errors, etc., which will contribute to the assembly error shown as the shaded beam in Fig. 4.

The displacements x_1 and x_2 represent the errors of the two horizontal beams in their assembly stations (fixture locator error and/or supporting part joint misallocation due to part fabrication). We refer to these as the process Key Control Characteristics (KCCs). The displacements z_1 and z_2 represent the product assembly dimensions. We refer to these as the Key Product Characteristics (KPCs), whose behaviors are dictated by product design requirements.

The governing equation of the assembly that relates the KPCs to the KCCs is given by

$$\begin{aligned} c_{11}x_1 + c_{12}x_2 &= z_1, \\ c_{21}x_1 + c_{22}x_2 &= z_2. \end{aligned} \tag{4}$$

The constants c_{11}, c_{12}, c_{21} and c_{22} may be obtained by evaluating the coefficients in Equations (1) and (2), details of which can be found in Shiu *et al.* (1997). More generally, with m KPC points and n KCC points, one can write the linearized model as

$$\mathbf{C}\mathbf{x} = \mathbf{z}, \tag{5}$$

where $\mathbf{z} = [z_1\ z_2 \ldots, z_m]^T$ is the vector of KPCs, $\mathbf{x} = [x_1\ x_2 \ldots x_n]^T$ is the vector of KCCs, and $\mathbf{C} = [\mathbf{c}_1\ \mathbf{c}_2 \ldots \mathbf{c}_m]^T$ is the matrix of coefficients with $\mathbf{c}_i = [c_{i1}\ c_{i2} \ldots c_{in}]$. Note that here, as in the remainder of the paper, all dimensions are referenced as deviations from design nominal.

4. Deterministic and stochastic interpretation of KPC constraints

In tolerance allocation, the goal is to specify the allowable tolerances for the KCC points $\{x_i\}_{i=1}^n$ based on the allowable tolerances for the KPC points $\{z_i\}_{i=1}^m$, which are assumed to be given and are based on the required functionality of the assembled product. For example, the set of KPCs on a chassis mounting surface of a vehicle have to be within certain tolerances in order to have proper wheel alignment. Denote the specified allowable tolerances for the KPCs as $\{T_{Z_i}\}_{i=1}^m$. Satisfying the KPC constraints means that the following must hold

$$|z_i| \leqslant T_{Z_i} : i = 1, 2, \ldots, m. \tag{6}$$

Using the linear model of Equation (5), the KPC constraints can be transformed into KCC coordinates via

$$|\mathbf{c}_i^T \mathbf{x}| \leqslant T_{Z_i} : i = 1, 2, \ldots, m. \tag{7}$$

Figure 5(a and b) graphically illustrates Equations (6) and (7). The KPC constraint region is rectangular in KPC coordinates, as shown in Fig. 5(a). In contrast, the KPC constraint region obtained from Equation (7) will not be rectangular in KCC coordinates in general, as shown in Fig. 5(b).

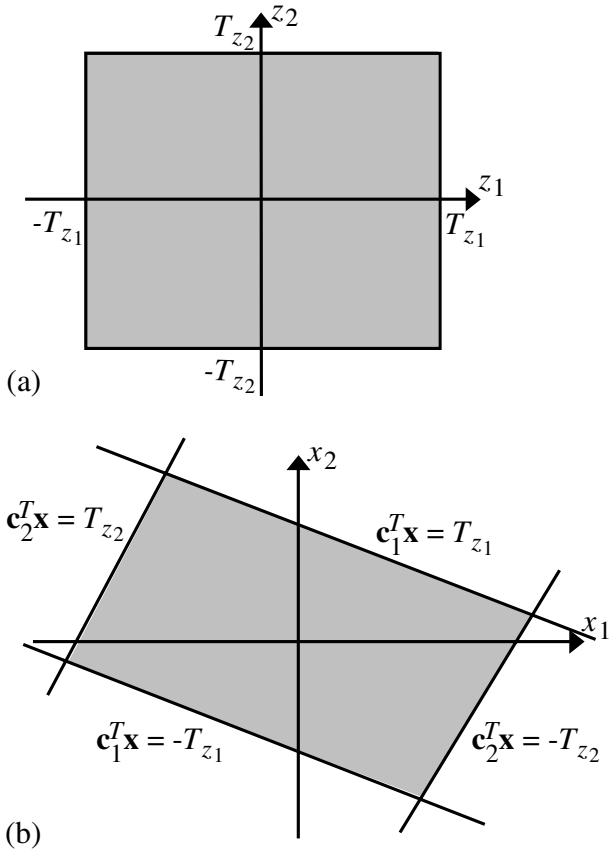

Fig. 5. Illustration of the KPC constraint region in: (a) KPC coordinates; and (b) KCC coordinates.

There are different interpretations of how to constrain (i.e., allocate tolerance to) the KCCs in order to achieve the constraints on the KPCs. One may view the KPCs and KCCs as deterministic variables and select the KCC tolerances so that the KPCs satisfy the KPC constraints deterministically (100% of the time). Alternatively, one may view the KPCs and KCCs as random variables and specify the KCC tolerances (e.g., in the form of $\pm 3\sigma$ variation limits) so that the KPCs satisfy the KPC constraints with a desired probability. Both interpretations are elaborated in the following subsections.

4.1. *Deterministic case*

Let T_{x_i} denote the allocated tolerance for x_i, so that the allowable range for x_i is the interval $[-T_{x_i}, T_{x_i}]$ and define $\mathbf{T_x} = [T_{x_i}, \ldots, T_{x_n}]$. Assuming the KCCs vary independently, $\boldsymbol{x}$ can then lie anywhere within the rectangular region of Fig. 6, which we refer to as the KCC tolerance region. Thus, if the KPC constraints are to be satisfied, we must specify $\mathbf{T_x}$, so that the rectangular KCC tolerance region lies within the KPC constraint region shown in Fig. 5(b).

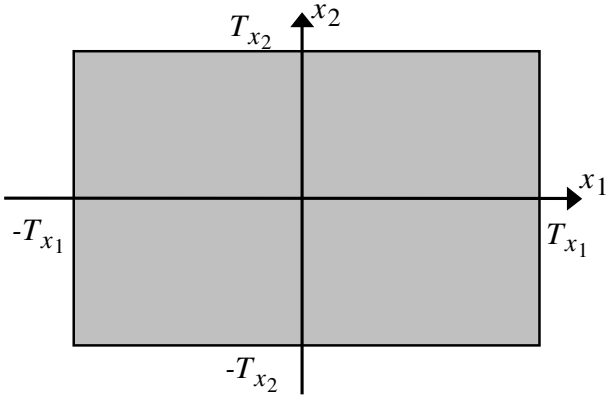

Fig. 6. Deterministic KCC tolerance region.

Two examples of KCC tolerancing schemes for which the KCC tolerance region lies within the KPC constraint region are illustrated in Fig. 7. Both tolerancing schemes satisfy the KPC constraints.

Since there are an infinite number of KCC tolerancing schemes for which the KPC constraints are satisfied, the tolerance allocation problem is how to "optimally" specify $\mathbf{T_x}$, under the constraint that the rectangular KCC tolerance region lies entirely within the KPC constraint region. One possible optimization criterion is to maximize the volume of the KCC tolerance region rectangle, or equivalently, minimize

$$F_1(\mathbf{T_x}) \equiv \prod_{i=1}^{n} \frac{1}{T_{x_i}}. \tag{8}$$

A draw back of this criterion is that it weights each x_i equally. One may wish to penalize more for assigning tighter tolerances to the x_i's that are more costly to control. Thus, a more attractive approach is to attempt to define the manufacturing costs of tight tolerances and minimize the cost. Popular cost functions are of the form

$$F_2(\mathbf{T_x}) \equiv \sum_{i=1}^{n} \frac{A_i}{(T_{x_i})^j}, \tag{9}$$

where the A_i are relative weights for the KCCs and j is some positive integer, e.g., one, two, three or four. Wu *et al.* (1988) and Chase *et al.* (1990) provide more detailed descriptions of these and other cost functions. The minimization is under the constraint that $|\boldsymbol{c}_i^T \boldsymbol{x}| \leqslant T_{z_i}$, for all $\mathbf{x}$ in the KCC tolerance region, as illustrated in Fig. 7.

4.2. *Stochastic interpretation*

Often, it is more appropriate to think of the x_i's as random variables and, instead of specifying "hard" tolerance

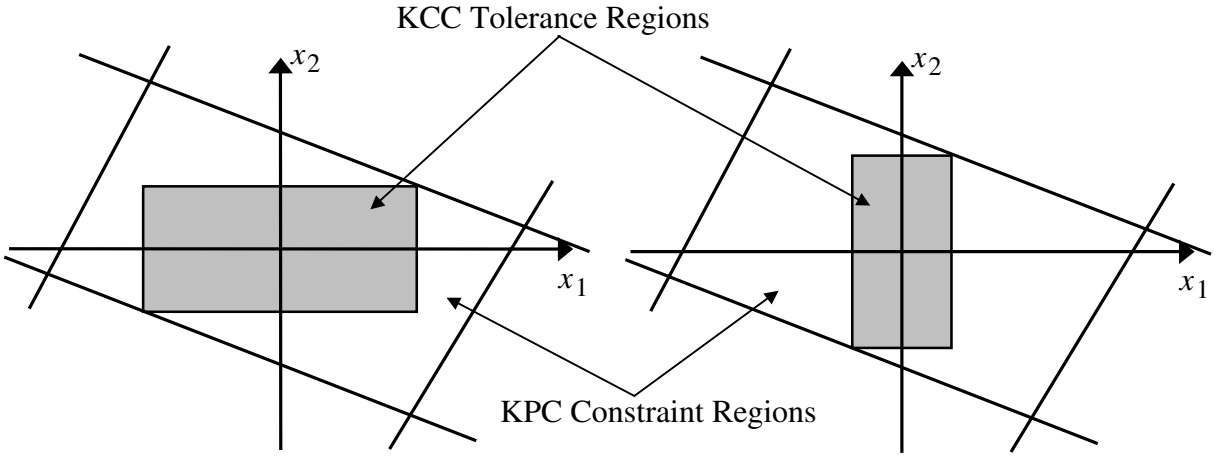

Fig. 7. Example of two KCC tolerancing schemes that satisfy the KPC constraints.

constraints on them, specify probabilistic constraints. Assuming all KCC variables are normally independently distributed, this amounts to appropriately specifying the standard deviation of each x_i, which we denote by σ_i. By making the σ_i's larger or smaller, one can control the probability that the KPC constraints are violated. In many cases the stochastic model is more appropriate, since the deterministic approach is usually overly conservative, as illustrated in Fig. 8. In Fig. 8 the rectangle associated with the larger tolerancing scheme would be rejected because the KPC constraints are violated. However, if x_1 and x_2 vary independently, there may be a negligibly small probability that they fall in the darkened regions lying outside the KPC constraint region. Additionally, the deterministic approach may not even be valid, since it may be impossible to guarantee that $|x_i| \leqslant T_{x_i}$ 100% of the time with no exceptions.

Assume that $x_i \sim \mathrm{NID}(0, \sigma_i^2)$, i.e., that the KCCs are normally, independently distributed with zero mean and standard deviation σ_i. The stochastic tolerance allocation task is to specify each σ_i (or $3\sigma_i$ limits for each x_i) such that the probability of lying outside the KPC constraint region is an acceptable specified small value, say α. Furthermore, the σ_i's are to be specified optimally in a manner that minimizes some appropriate cost function. This approach has been considered in Lee and Woo (1990). One difficulty is that given $\{\sigma_i\}_{i=1}^n$, it is difficult to calculate the exact probability of lying outside the KPC constraint region. In contrast, it is quite easy to come up with an upper bound on this probability using ellipsoids that are contained within the KPC constraint region.

To illustrate, suppose we have a stochastic KCC tolerance vector $\boldsymbol{\sigma} \equiv [\sigma_1^2\ \sigma_2^2 \ldots \sigma_n^2]^T$, and define

$$\boldsymbol{\Sigma} \equiv \mathrm{diag}\left\{\frac{1}{\sigma_1^2}, \frac{1}{\sigma_2^2}, \ldots, \frac{1}{\sigma_n^2}\right\}.$$

Consider the ellipsoid $\boldsymbol{x}^T\boldsymbol{\Sigma}\boldsymbol{x} = K$ for some arbitrary positive constant K. If the σ_i are made small enough, we can ensure that the ellipsoid is contained inside the KPC constraint region as illustrated in Fig. 9. If this is the case, then the probability that $\boldsymbol{x}$ falls outside the KPC constraint region is less than or equal to the probability that $\mathbf{x}$ falls outside the ellipsoid.

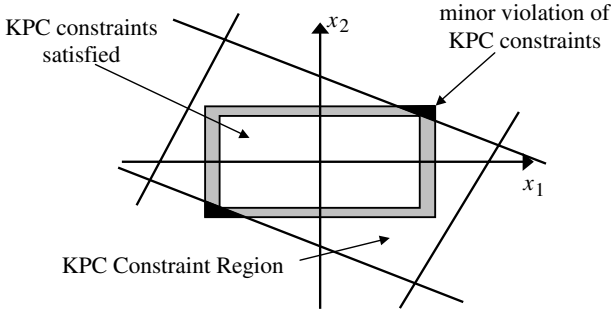

Fig. 8. Illustration of the conservative nature of the deterministic approach.

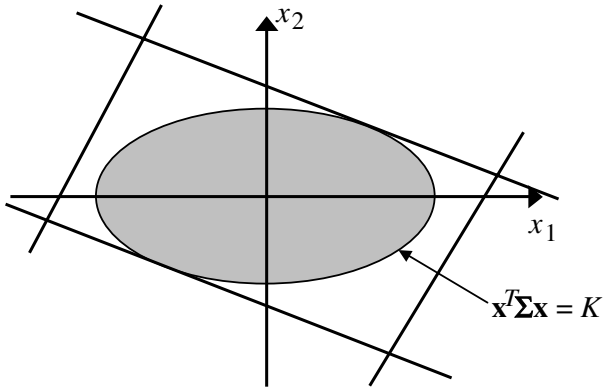

Fig. 9. Acceptable conditions.

The probability that $\boldsymbol{x}$ lies outside the ellipsoid $\boldsymbol{x}^T\boldsymbol{\Sigma}\boldsymbol{x} = K$ is exactly α if the constant K is chosen to be 1-α percentile of the $\chi^2(n)$ distribution, i.e., the χ^2 distribution with n degrees of freedom. This follows by noting that

$$\boldsymbol{x}^T\boldsymbol{\Sigma}\boldsymbol{x} = \sum_{i=1} \frac{x_i^2}{\sigma_i^2}, \tag{10}$$

which is a $\chi^2(n)$ random variable. Thus the probability that $\boldsymbol{x}$ lies outside the ellipsoid is:

$$\Pr[\boldsymbol{x}^T\boldsymbol{\Sigma}\boldsymbol{x} > K] = \Pr[\chi^2(n) > K] \equiv \alpha. \tag{11}$$

Hence, if the σ_i's are small enough so that the ellipsoid is contained within the KPC constraint region, α is an upper bound on the probability of violating a KPC constraint.

In general, the larger the σ_i's are, the closer the upper bound α is to the true probability of violating a KPC constraint. This coincides with the goals of choosing the σ_i's to minimize a manufacturing cost function, since manufacturing cost will always decrease as the σ_i's increase.

This suggests a procedure for optimally allocating tolerances (i.e., choosing the σ_i's) that guarantees the probability that one or more of the KPC constraints are violated is less than α: Set K to be the 1-α percentile of the $\chi^2(n)$ distribution, and choose the σ_i's so that the ellipsoid $\boldsymbol{x}^T\boldsymbol{\Sigma}\boldsymbol{x} = K$ is as large as possible (in the sense of minimizing one of the cost functions below) while still being contained entirely within the KPC constraint region.

Similarly to the deterministic case, one could minimize the cost function

$$F_1(\boldsymbol{\sigma}) \equiv \prod_{i=1}^{n} \frac{1}{\sigma_i}, \tag{12}$$

which is inversely proportional to the ellipsoid volume. Alternatively, one may use a cost function of the form,

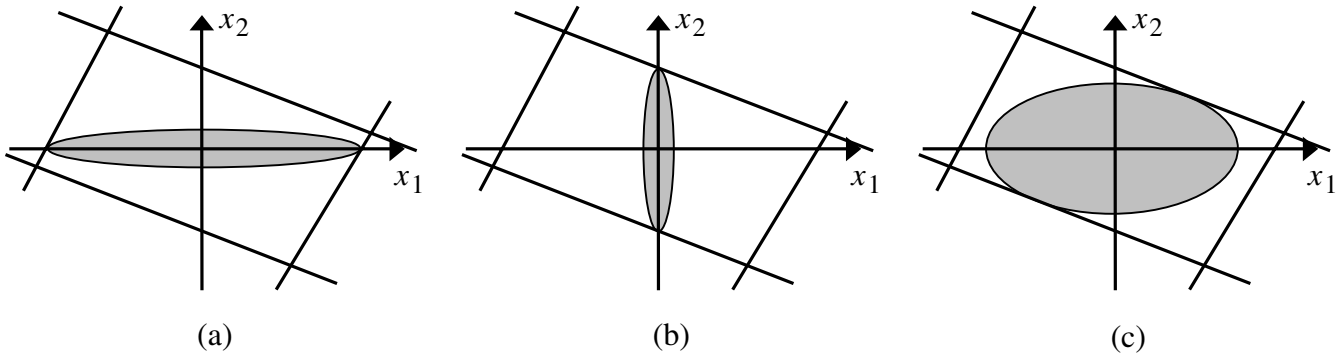

Fig. 10. Tolerancing schemes satisfying the probabilistic constraints, but with different costs: (a) high cost; (b) high cost; (c) lower cost.

$$F_2(\boldsymbol{\sigma}) \equiv \sum_{i=1}^{n} \frac{A_i}{(\sigma_i)^j}, \tag{13}$$

so that different KCCs can be weighted differently. Here, we can chose $i = 1, 2, 3, 4, \ldots$ etc. The optimal stochastic tolerance allocation is illustrated in Fig. 10(a–c), which shows three different tolerancing schemes each satisfying the constraints but with different costs.

5. Reformulation of the constraints

Other authors have proposed similar optimal tolerancing concepts (e.g. Lee and Woo (1990) for the stochastic interpretation problem). See Chase and Parkinson (1991) for a survey of these methods. In their present form, however, the constraints that the ellipsoid defined by $\boldsymbol{\sigma}$ (stochastic case) and the rectangle defined by $\mathbf{T_x}$ (deterministic case) lie within the KCC constraint region are not easy to work with and the resulting optimization algorithms are complicated. In this section, we show that the constraints can be reformulated into a very manageable form so that the resulting optimization problem is simple and can be easily solved using standard optimization packages. Moreover, the constraint equations have exactly the same form for both the deterministic and the stochastic approaches.

5.1. *Stochastic case*

For the stochastic interpretation, the optimization criterion is expressed in terms of $\boldsymbol{\sigma}$. We would also like to express as a simple function of $\boldsymbol{\sigma}$, the constraint that the ellipsoid $\boldsymbol{x}^T\boldsymbol{\Sigma}\boldsymbol{x} = K$ lies within the KPC constraint region.

Consider the ith KPC constraint $|\boldsymbol{c}_i^T\boldsymbol{x}| \leqslant T_{Z_i}$. By symmetry of both the constraint and the ellipsoid, we need only consider the constraint $\boldsymbol{c}_i^T\boldsymbol{x} \leqslant T_{Z_i}$. Rewrite this as $\boldsymbol{y}_i^T\boldsymbol{x} \leqslant 1$ where $\boldsymbol{y}_i \equiv \boldsymbol{c}_i/T_{Z_i}$. The optimization problem is to find the $\boldsymbol{\sigma}$ that minimizes the cost function $F(\boldsymbol{\sigma})$ subject to the constraints $\boldsymbol{y}_i^T\boldsymbol{x} \leqslant 1$ ($i = 1$ to m) for all $\boldsymbol{x}$ on and within the ellipsoid $\boldsymbol{x}^T\boldsymbol{\Sigma}\boldsymbol{x} = K$.

Given an arbitrary $\boldsymbol{\sigma}$ and K, all points $\boldsymbol{x}$ on and within the ellipsoid $\boldsymbol{x}^T\boldsymbol{\Sigma}\boldsymbol{x} = K$ satisfy the ith constraint $\boldsymbol{y}_i^T\boldsymbol{x} \leqslant 1$ iff the hyperplane $S_i \equiv \{\boldsymbol{x}|\boldsymbol{y}_i^T\boldsymbol{x} = 1\}$ lies outside the ellipsoid. This, in turn, is true iff $\boldsymbol{x}^T\boldsymbol{\Sigma}\boldsymbol{x} \geqslant K\ \forall \boldsymbol{x} \in S_i$. Since $\Re^n$ with inner product $\langle \boldsymbol{x}|\boldsymbol{y}\rangle_{\boldsymbol{\Sigma}} \equiv \boldsymbol{x}^T\boldsymbol{\Sigma}\boldsymbol{y}$ is a valid Hilbert space with norm $\|\boldsymbol{x}\|_{\boldsymbol{\Sigma}} \equiv \sqrt{\langle \boldsymbol{x}|\boldsymbol{x}\rangle_{\boldsymbol{\Sigma}}} = \sqrt{\boldsymbol{x}^T\boldsymbol{\Sigma}\boldsymbol{x}}$, this last condition is true iff

$$\inf_{X \in s_i} \|\boldsymbol{x}\|_{\boldsymbol{\Sigma}} \geqslant \sqrt{K}.$$

Define

$$\boldsymbol{v}_i = \arg\min_{\boldsymbol{x} \in s_i} \|\boldsymbol{x}\|_{\boldsymbol{\Sigma}},$$

i.e., $\boldsymbol{v}_i$ is the point on S_i with smallest $\boldsymbol{\Sigma}$-norm, as illustrated in Fig. 11.

To find $\boldsymbol{v}_i$, note that S_i can be represented as

$$S_i = \{\boldsymbol{x}|\boldsymbol{y}_i^T\boldsymbol{x} = 1\} = \{\boldsymbol{x}|\boldsymbol{y}_i^T\boldsymbol{\Sigma}^{-1}\boldsymbol{\Sigma}\boldsymbol{x} = 1\} = \{\boldsymbol{x}|w_i^T\boldsymbol{\Sigma}\boldsymbol{x} = 1\}$$
$$= \{\boldsymbol{x}|\langle \boldsymbol{w}_i|\boldsymbol{x}\rangle_{\boldsymbol{\Sigma}} = 1\},$$

where $\boldsymbol{w}_i \equiv \boldsymbol{\Sigma}^{-1}\boldsymbol{y}_i$. Thus, S_i is a hyperplane generated from an inner product constraint. As a result, the classical projection theorem (Luenberger, 1997) implies that

$$\boldsymbol{v}_i = \boldsymbol{\beta}_i \boldsymbol{w}_i, \tag{14}$$

where

$$\boldsymbol{\beta}_i \equiv \frac{1}{\langle \boldsymbol{w}_i|\boldsymbol{w}_i\rangle_{\boldsymbol{\Sigma}}} = \frac{1}{\boldsymbol{w}_i^T\boldsymbol{\Sigma}\boldsymbol{w}_i} = \frac{1}{\boldsymbol{y}_i^T\boldsymbol{\Sigma}^{-1}\boldsymbol{\Sigma}\boldsymbol{\Sigma}^{-1}\boldsymbol{y}_i} = \frac{1}{\boldsymbol{y}_i^T\boldsymbol{\Sigma}^{-1}\boldsymbol{y}_i}. \tag{15}$$

Therefore,

$$\boldsymbol{v}_i = \frac{\boldsymbol{\Sigma}^{-1}\boldsymbol{y}_i}{\boldsymbol{y}_i^T\boldsymbol{\Sigma}^{-1}\boldsymbol{y}_i},$$

and

$$\|\boldsymbol{v}_i\| = \sqrt{\boldsymbol{v}_i^T\boldsymbol{\Sigma}\boldsymbol{v}_i} = \sqrt{\frac{\boldsymbol{y}_i^T\boldsymbol{\Sigma}^{-1}\boldsymbol{\Sigma}\boldsymbol{\Sigma}^{-1}\boldsymbol{y}_i}{(\boldsymbol{y}_i^T\boldsymbol{\Sigma}^{-1}\boldsymbol{y}_i)^2}} = \sqrt{\frac{1}{\boldsymbol{y}_i^T\boldsymbol{\Sigma}^{-1}\boldsymbol{y}_i}}.$$

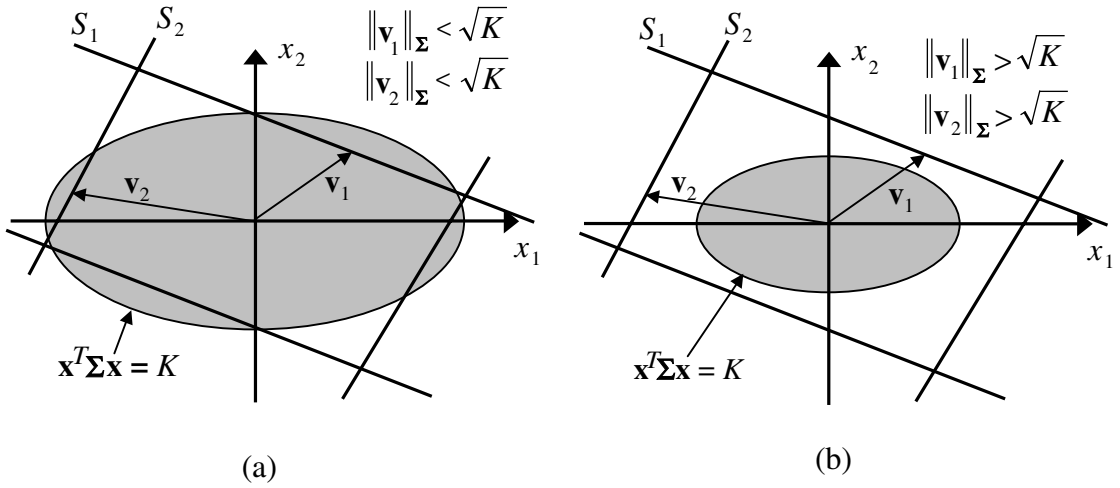

Fig. 11. (a) A $\mathbf{\Sigma}$ such that the ellipsoid violates the KPC constraints; and (b) a $\mathbf{\Sigma}$ such that the ellipsoid satisfies the KPC constraints.

Consequently, all points on and within the ellipsoid $\boldsymbol{x}^T\mathbf{\Sigma}\boldsymbol{x} = K$ satisfy the ith constraint $\left|\boldsymbol{y}_i^T\boldsymbol{x}\right| \leqslant 1$ iff

$$\|\boldsymbol{v}_i\|_{\mathbf{\Sigma}} \geqslant \sqrt{K} \Leftrightarrow \frac{1}{\boldsymbol{y}_i^T\mathbf{\Sigma}^{-1}\boldsymbol{y}_i} \geqslant K \Leftrightarrow \boldsymbol{y}_i^T\mathbf{\Sigma}^{-1}\boldsymbol{y}_i \leqslant \frac{1}{K}$$
$$\Leftrightarrow \sum_{j=1}^{n} \boldsymbol{y}_{i,j}^2\boldsymbol{\sigma}_j^2 \leqslant \frac{1}{K} \Leftrightarrow \bar{\boldsymbol{y}}_i^T\boldsymbol{\sigma} \leqslant \frac{1}{K}, \tag{16}$$

where $\overline{\boldsymbol{y}_i} \equiv [\boldsymbol{y}_{i,1}^2\boldsymbol{y}_{i,2}^2 \cdots \boldsymbol{y}_{i,n}^2]^T$, and $\boldsymbol{y}_{i,j}$ is the jth element of $\boldsymbol{y}_i$.

Figure 11 (a and b) illustrates two cases. In Fig. 11(b) the ellipsoid lies within the constraint region since $\|\boldsymbol{v}_1\|_{\mathbf{\Sigma}} \geqslant \sqrt{K}$, and $\|\boldsymbol{v}_2\|_{\mathbf{\Sigma}} \geqslant \sqrt{K}$. In Fig. 11(a) the ellipsoid violates both constraints since $\|\boldsymbol{v}_1\|_{\mathbf{\Sigma}} < \sqrt{K}$ and $\|\boldsymbol{v}_2\|_{\mathbf{\Sigma}} < \sqrt{K}$.

The significance of Equation (16) is that the KCC constraint region within which the ellipsoid lies, and which is non-linear in x-coordinates, has been transformed into a set of constraints that are linear in σ-coordinates. The optimal tolerance allocation problem for the stochastic case then becomes

$$\min F(\boldsymbol{\sigma}), \tag{17}$$

subject to

$$\overline{\boldsymbol{y}_i}^T\boldsymbol{\sigma} \leqslant \frac{1}{K} \ (i = 1, 2, \ldots, m), \tag{18}$$

$$\sigma_i \geqslant 0 \ (i = 1, 2, \ldots m). \tag{19}$$

The optimization problem is illustrated in Fig. 12. Since the constraints are linear and the constraint region is convex, the optimization problem can be easily and robustly solved using standard optimization packages, e.g. Matlab. Note that the constraint vectors $\bar{\boldsymbol{y}}_i$ have all non-negative elements.

5.2. *Deterministic case*

For the deterministic case, the constraint that the rectangular region defined by $|x_i| \leqslant T_{xi}$ $(i = 1, 2, \ldots n)$ lies within the KPC constraint region can be transformed into a form that is nearly identical to the ellipsoidal constraint for the stochastic case. First, note that the rectangle lies within the KPC constraint region iff all of its vertices do, and all 2^n vertices will be of the form $\boldsymbol{x} = [\pm T_{x_1} \pm T_{x_2} \ldots \pm T_{x_n}]^T$. Thus, the ith KPC constraint $\left|\boldsymbol{y}_i^T\boldsymbol{x}\right| \leqslant 1$, will be satisfied by all vertices iff

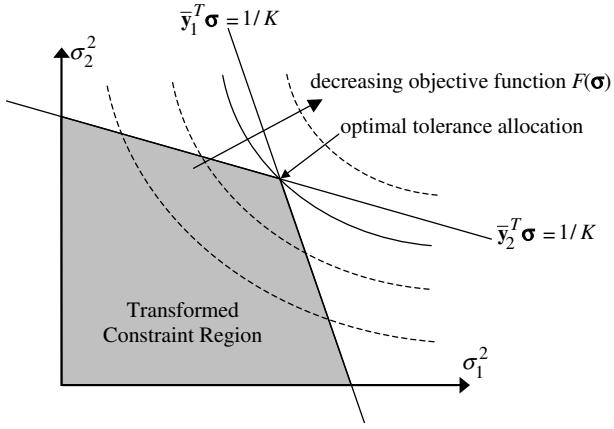

Fig. 12. Converted optimization space.

$$\overline{\boldsymbol{y}_i}^T\mathbf{T}_{\mathbf{x}} \leqslant 1, \tag{20}$$

where we have re-defined $\overline{\boldsymbol{y}_i} \equiv [|\boldsymbol{y}_{i,1}||\boldsymbol{y}_{i,2}| \ldots |\boldsymbol{y}_{i,n}|]^T$ and $\mathbf{T}_{\mathbf{x}} = [T_{x_1} T_{x_2} \ldots T_{x_n}]^T$.

Thus, the constraints on $\mathbf{T}_{\mathbf{x}}$ for the deterministic tolerance allocation case are of the exact same linear form as the constraints on $\boldsymbol{\sigma}$ in the stochastic tolerance allocation case. The only difference is that for the stochastic case $\overline{\boldsymbol{y}_i} \equiv [y_{i,1}^2 y_{i,2}^2 \ldots y_{i,n}^2]^T$, whereas, for the deterministic case $\overline{\boldsymbol{y}_i} \equiv [|y_{i,1}||y_{i,2}| \ldots |y_{i,n}|]^T$. Note that for both cases the elements of the constraint vectors $\{\overline{\boldsymbol{y}_i}\}_{i=1}^m$ are non-negative. The optimization problem for the deterministic case is also represented by Fig. 12, if $\boldsymbol{\sigma}$ is replaced by $\mathbf{T}_{\mathbf{x}}$.

6. Implementation procedure and case study

The optimal tolerancing algorithm is summarized as follows:

Step 1. Formulate the linear or linearized model relating the KPCs to the KCCs $z_i = \boldsymbol{c}_i^T \boldsymbol{x} (i = 1, 2, \ldots, m)$ and specify tolerance on each of the KPCs $|z_i| \leqslant T_{z_i} (i = 1, 2, \ldots, m)$.

Step 2. For $i = 1, 2, \ldots, m$, define $\boldsymbol{y}_i \equiv \boldsymbol{c}_i / T_{z_i}$ and set $\overline{\boldsymbol{y}_i} \equiv [y_{i,1}^2 y_{i,2}^2 \ldots y_{i,n}^2]^T$ for the stochastic case. $\overline{\boldsymbol{y}_i} \equiv [|y_{i,1}||y_{i,2}| \ldots |y_{i,n}|]^T$ for the deterministic case.

Step 3. Select the most appropriate cost function: $F(\boldsymbol{\sigma})$ for the stochastic case, or $F(\mathbf{T_x})$ for the deterministic case.

Step 4. (a) **Stochastic case**; select α (the algorithm ensures that the probability of violating one or more KPC constraints is no larger than α) and set K equal to the 1-α percentile of the $\chi^2(n)$ distribution. Minimize $F(\boldsymbol{\sigma})$ subject to $\overline{\boldsymbol{y}}^T \boldsymbol{\sigma} \leqslant 1/K$ $(i = 1, 2, \ldots, m)$ and $\sigma_i > 0$ $(i = 1, 2, \ldots, n)$

The ith element of the optimal $\boldsymbol{\sigma}$ is the allocated variance of x_i.

(b) **Deterministic case**; minimize $F(\mathbf{T_x})$ subject to $\overline{\boldsymbol{y}}^T \mathbf{T_x} \leqslant 1$ $(i = 1, 2, \ldots, m)$ and $\mathbf{T_x} > 0$ $(i = 1, 2, \ldots, n)$

The ith element of $\mathbf{T_x}$ is the allocated hard tolerance of x_i.

A three-dimensional experimental case study is provided below. A two-dimensional example is also provided to illustrate how different choices for the cost function influence the shape of the optimal ellipsoid and, hence, the optimal tolerance allocation.

6.1. *Experimental verification*

An experimental three-beam assembly depicted in Fig. 13 was constructed to verify the beam-based modeling and tolerance allocation methodology. The elements of the three-length KPC vector $\mathbf{z}$ are the x-, y-, and z-coordinates, respectively, of the joined end (node 1) of the three beam members. The three-length KCC vector $\mathbf{x}$ consists of the deviation from nominal of the lengths of beams 21, 31, and 41, respectively, and represents fabrication errors. In the experiment, this fabrication error was introduced by adding shims at the base ends (nodes 2, 3, and 4) of the three beams.

Considering the geometry of the assembly and using the procedures described in the earlier sections, the model relating the KPCs to the KCCs is

$$\begin{bmatrix} z_1 \\ z_2 \\ z_3 \end{bmatrix} = \begin{bmatrix} 0.707 & 0.707 & 0 \\ 0.707 & 0.707 & -1.414 \\ -0.707 & 0.707 & 0 \end{bmatrix} \begin{bmatrix} x_1 \\ x_2 \\ x_3 \end{bmatrix}. \qquad (21)$$

Suppose the three KPCs are each assigned tolerances of ± 2.89 mm and that the cost function shown in Equation (12) is chosen so as to maximize the ellipsoidal volume. If $\alpha = 0.01$ is selected, this results in $K = 11.34$, the 0.99 percentile of the χ^2 distribution with three degrees-of-freedom. Numerical optimization using the methods described in previous sections results in allocating tolerances of $\sigma_1 = 0.701$, $\sigma_2 = 0.701$, and $\sigma_3 = 0.350$ to the three KCCs. The optimal ellipsoid is $(x_1/\sigma_1)^2 + (x_2/\sigma_2)^2 + (x_3/\sigma_3)^2 = K$ or, equivalently, $(x_1/2.36)^2 + (x_2/2.36)^2 + (x_3/1.18)^2 = 1$. This ellipsoid intersects the x_1, x_2, and x_3 axes at ± 2.36, ± 2.36, and ± 1.18, respectively. It can be verified that the ellipsoid lies strictly inside the S_1 and S_3 planes, but just touches the S_2 plane at the point $\mathbf{v}_2 = [1.36\ 1.36 - 0.68]^T$. Note that the equa-

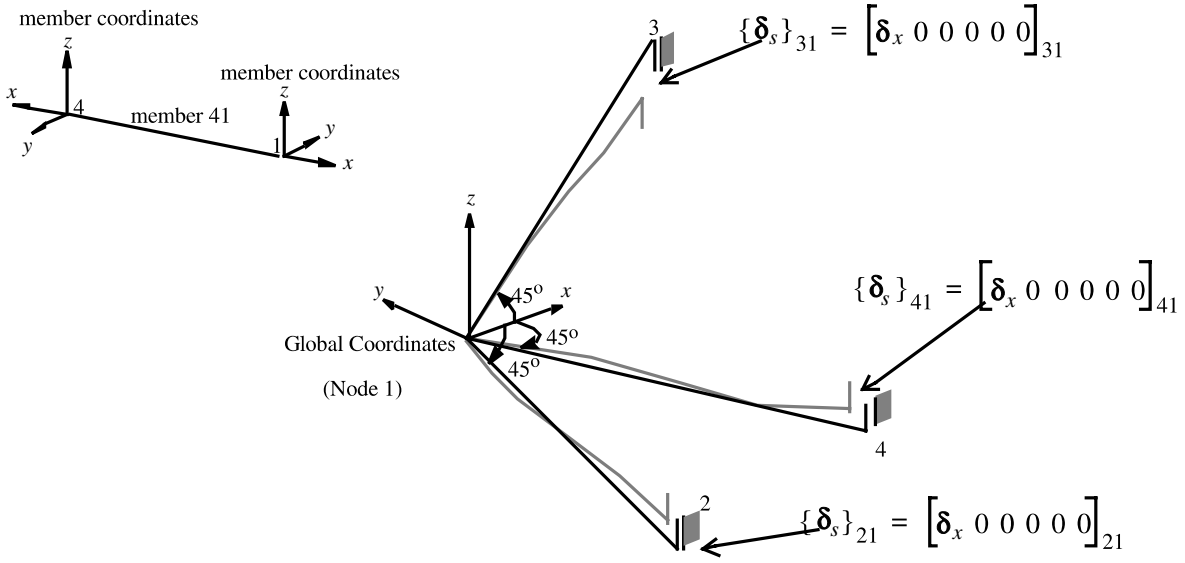

Fig. 13. Experimental assembly.

tions for the S_1, S_2, and S_3 planes are the three rows of Equation (21), with z_1, z_2, and z_3 each set to their assigned tolerances of 2.89 mm.

Suppose, instead, that one wished to allocate tolerances deterministically using the cost function (8), so as to maximize the rectangular volume. In this case, using the methods described in previous sections results in allocating deterministic tolerances of $T_{x_1} = 1.36, T_{x_2} = 1.36$, and $T_{x_3} = 0.68$ to the three KCCs. It is interesting to note that this rectangle is contained entirely within the optimal ellipsoid for the stochastic case, with the two touching at the vertices $[\pm 1.36 \ \pm 1.36 \ \pm 0.68]^T$. This illustrates the overly conservative nature of the deterministic approach: if the deterministic approach is used, one attempts to control the KCC to lie within the relatively small rectangle. In contrast, if the stochastic approach is used, one only attempts to control the KCCs to lie within (with probability 0.99) the much larger ellipsoid.

To verify the effectiveness of the beam-based model and tolerance allocation methodology, the following experiment was conducted on the experimental assembly depicted in Fig. 13. Over each of 14 experimental runs, shims of various thickness were added/removed at the base of the three beam members to represent fabrication errors in their lengths. The net increase/decrease in their lengths for each run are listed as the KCC values in Table 1. The table also shows the predicted values using Equation (21) and the observed experimental values of the KPCs for each run. Each run was replicated five times, and the observed KPC values shown are the average of the five replicates. The numbers in parentheses are the 6σ values for the five replicates. The variability in the replicates was due to a combination of measurement error, modeling approximations, and errors in the shim thicknesses. The KCC combinations throughout the experiment were all chosen to fall within the optimal ellipsoid $(x_1/2.36)^2 + (x_2/2.36)^2 + (x_3/1.18)^2 = 1$. As the model predicts, all of the observed KPC values satisfied the KPC tolerance constraints $|z_i| \leqslant 2.89$.

6.2. *Effects of varying the cost function*

As mentioned previously, there are a number of different cost functions that may be considered, examples of which are shown in Table 2.

In Table 2, k_i, k, A_i may be chosen so that each tolerance carries different weight in the overall manufacturing cost. To illustrate the effects of changing the weights, consider the cost functions

$$F_1(\boldsymbol{\sigma}) = \frac{2}{\sigma_1} + \frac{1}{\sigma_2}, \ F_2(\boldsymbol{\sigma}) = \frac{1}{\sigma_1} + \frac{1}{\sigma_2}, \text{ and } F_3(\boldsymbol{\sigma}) = \frac{1}{\sigma_1} + \frac{2}{\sigma_2}.$$

The optimal ellipses for these three cost functions are shown in Fig. 14(a), where the two constraint surfaces that were assumed are also shown. Clearly, the weight assigned to each KCC tolerance in the cost function affects the shape of the optimal ellipse and hence, the optimal tolerance assignment. For example, assigning tight tolerance to x_1 incurs more cost than assigning tight tolerance to x_2 when $F_1(\boldsymbol{\sigma})$ is assumed. The converse is true when $F_3(\boldsymbol{\sigma})$ is assumed. Consequently, relative to the optimally allocated σ_2, the optimally allocated σ_1 would be larger for $F_1(\boldsymbol{\sigma})$ than for $F_3(\boldsymbol{\sigma})$. This is evident from Fig. 14(a), in which the optimal ellipsoid for $F_1(\boldsymbol{\sigma})$ is stretched longer in the x_1 direction than is the optimal ellipsoid for $F_3(\boldsymbol{\sigma})$.

Similar conclusions apply when the cost functions $F_4(\boldsymbol{\sigma}) = \sigma_1^{-1}\sigma_2^{-1}$, $F_5(\boldsymbol{\sigma}) = \sigma_1^{-4}\sigma_2^{-1}$, and $F_6(\boldsymbol{\sigma}) = \sigma_1^{-1}\sigma_2^{-4}$ are

Table 1. Experimental results for tolerance prediction and allocation

Run	*KCC values*			*KPC values*					
	x_1	x_2	x_3	*Predicted*			*Experimental*		
				z_1	z_2	z_3	z_1	z_2	z_3
1	2.37	0.00	0.00	1.68	1.68	−1.68	1.64(0.16)	1.46(0.71)	−1.59(0.34)
2	−2.37	0.00	0.00	−1.68	−1.68	1.68	−1.66(0.98)	−1.93(1.01)	1.72(1.04)
3	0.00	2.37	0.00	1.68	1.68	1.68	1.70(0.66)	1.42(1.21)	1.71(0.61)
4	0.00	−2.37	0.00	−1.68	−1.68	−1.68	−1.75(0.47)	−2.17(0.77)	−1.86(2.51)
5	0.00	0.00	1.18	0.00	−1.67	0.00	−0.01(0.68)	−2.01(0.50)	0.16(0.50)
6	0.00	0.00	−1.18	0.00	1.67	0.00	0.10(0.65)	1.41(1.21)	0.09(0.65)
7	1.36	1.36	0.68	1.92	0.96	0.00	1.75(0.43)	0.16(0.81)	−0.02(0.44)
8	1.36	1.36	−0.68	1.92	2.88	0.00	1.75(0.34)	2.04(1.25)	0.02(0.25)
9	1.36	−1.36	−0.68	0.00	0.96	−1.92	0.04(0.40)	0.34(0.70)	−1.63(0.36)
10	1.36	−1.36	0.68	0.00	−0.96	−1.92	0.07(0.40)	−1.69(0.65)	−1.73(0.67)
11	−1.36	1.36	0.68	0.00	−0.96	1.92	0.05(0.62)	−1.64(0.70)	1.77(0.47)
12	−1.36	1.36	−0.68	0.00	0.96	1.92	0.07(0.60)	0.36(0.92)	1.78(0.25)
13	−1.36	−1.36	−0.68	−1.92	−0.96	0.00	−1.70(0.45)	−1.56(1.35)	0.02(0.42)
14	−1.36	−1.36	0.68	−1.92	−2.88	0.00	−1.58(0.37)	−2.04(1.25)	0.11(0.78)

Table 2. Different cost functions

Generalized cost function	*Generalized volume function*
$F(\sigma) = \sum_{i=1}^{n} \frac{A_i}{\sigma_i^k}$	$F(\sigma) = \prod_{i=1}^{n} \frac{1}{\sigma_i^{k_i}}$

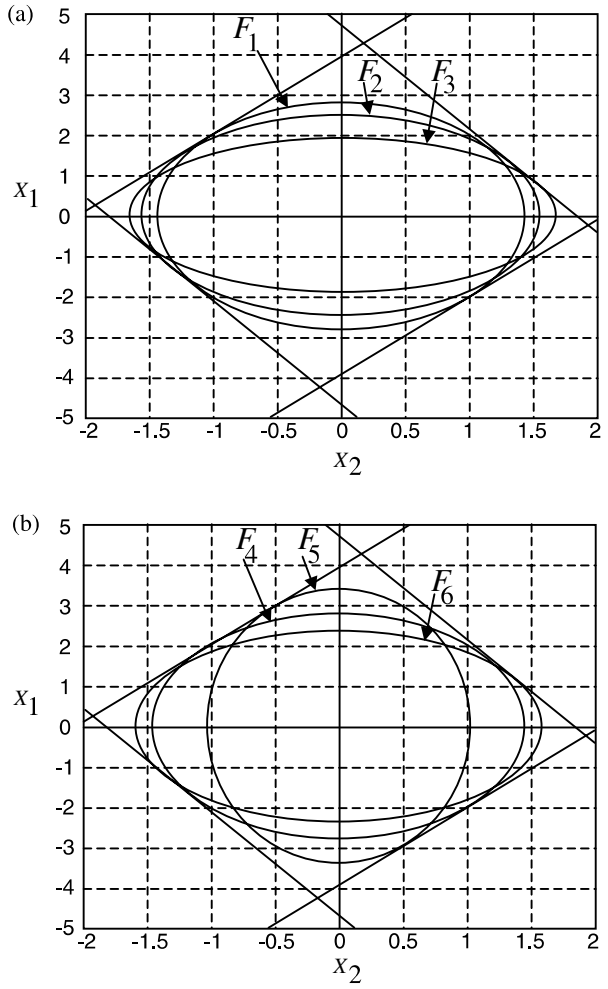

Fig. 14. Objective function comparison for: (a) F_1, F_2 and F_3; and (b) F_4, F_5 and F_6.

compared. The optimal ellipses for these cost functions are shown in Fig. 14(b). When tight tolerance on x_1 is more costly (i.e., for $F_5(\boldsymbol{\sigma})$), the optimal allocated σ_1 increases relative to the optimal allocated σ_2, and the optimal ellipse is elongated in the x_1 direction and contracted in the x_2 direction.

7. Conclusions

In order to properly allocate tolerances for modern complex products made of compliant parts (e.g., sheet metal assemblies such as automotive bodies, airplane fuselages, or household appliances), it is necessary to predict the effects of part and process variation on final product quality during the early stages of design. In general, existing approaches to allocating tolerances:

1. require detailed knowledge of final product geometry and thus, are applicable primarily during advanced stages of the design, which leads to a less than optimal design process; and
2. consider only rigid body characteristics of parts.

This paper addresses these limitations and presents a tolerance allocation methodology for compliant assemblies based on a beam structure model. The method is reasonably generic and can be applied to a broad class of assembly processes for compliant parts. The compliant beam structure model of the product does not require detailed knowledge of product geometry and thus, can be applied during the early design stages to develop cost-effective product specifications. The proposed method minimizes manufacturing costs associated with tolerances of critical process requirements (Key Control Characteristics (KCCs)) under the constraint of satisfying product functionality (represented as Key Product Characteristics (KPCs)). Misalignments and fabrication errors of compliant parts, two critical causes of product dimensional variation, are discussed and included in the model. The proposed methodology applies with either a stochastic or a deterministic interpretation of allocated manufacturing tolerances. An easily implemented optimization procedure for allocating tolerances was developed using classical projection theory to reformulate the tolerance constraints into a much more manageable form. The non-linear constraints, that ellipsoid defined by $\boldsymbol{\sigma}$ (stochastic case) or rectangle defined by $\mathbf{T_x}$ (deterministic case) lie within KCC region, are transformed into a set of constraints that are linear in $\boldsymbol{\sigma}$ (or $\mathbf{T_x}$)-coordinates. Standard optimization packages can then be used to solve the problem. It was also shown that the reformulated constraint equations have exactly the same form for both the deterministic approach and the stochastic approach. Experimental results verify the proposed tolerance allocation method.

References

Anderson, C.B. (1990) General system for least cost tolerance allocation in mechanical assemblies. ADCATS Reports No. 90-2, Brigham Young University, Salt Lake City, UT.

Bjorke, O. (1989) *Computer Aided Tolerancing*, Tapir Publishers, Trondheim, Norway.

Ceglarek, D. and Shi, J. (1995) Dimensional variation reduction for automotive body assembly. *Manufacturing Review*, **8**, 139–154.

Ceglarek, D. and Shi, J. (1996) Fixture Failure Diagnosis for the Autobody Assembly Using Pattern Recognition. *Transactions of the ASME: Journal of Engineering for Industry*, **118**(1), 55–66.

Ceglarek, D. and Shi, J. (1997) Tolerance analysis for sheet metal assembly using a beam-based model. *ASME Design Engineering Division Publication*, **94**, 153–159.

Ceglarek, D., Shi, J. and Wu, S.M. (1994) A knowledge-based diagnostic approach for the launch of the auto-body assembly process. *Transactions of the ASME: Journal of Engineering for Industry*, **116**, 491–499.

Chase, K.W., Greenwood, W.H., Loosli, B.G. and Hauglund, L.F. (1990) Least cost tolerance allocation for mechanical assemblies with automated process selection. *Manufacturing Review*, **3**(1), 49–59.

Chase, K.W. and Parkinson, A.R. (1991) A survey of research in the application of tolerance analysis to the design of mechanical assemblies. *Research in Engineering Design*, **3**, 23–37.

Chon, C.T., Mohammadtorab, H. and El-Essawi, M. (1986) Generic stick model of a vehicular structure. SAE Paper 860825.

Choudhuri, S.A. and DeMeter, E.C. (1999) Tolerance analysis of machining fixture locators. *Transactions of the ASME: Journal of Manufacturing Science and Engineering*, **121**, 273–281.

Eggert, R.J. and Mayne, R.W. (1990) Probabilistic optimization using successive surrogate probability density functions, in *Proceedings of the ASME 16th Design Automation Conference*, DE-**23**(1), 129–134.

Etesami, F. (1993) Mathematical model for geometric tolerances. *Transactions of the ASME: Journal of Mechanical Design*, **115**(1), 81–86.

Faux, I.D. (1986) Reconciliation of Design and Manufacturing Requirements for Product Description Data Using Functional Primitive Part Features, CAM-1 Report No. R-86-ANC/GM/PP 01.1, CAM-1 Inc., Arlington, TX.

Guilford, J. and Turner, J. (1993) Advanced tolerance analysis and synthesis for geometric tolerances. *ASME International Forum on Dimensional Tolerancing and Metrology*, CRTD **27**, 187–198.

Hong, Y.S. and Chang, T.-C. (2002) A Comprehensive Review of Tolerancing Research. *International Journal of Production Research*, **40**(11), 2425–2459.

Hillyard, R.C. and Braid, I.C. (1978) Analysis of dimensions and tolerances in computer-aided mechanical design. *Computer Aided Design* **10**, 161–166.

Jastrzebski, M.J. (1991) Software for analysis of three dimensional statistical tolerance propagation in assemblies using closed form matrix transforms. MSc Paper, Massachusetts Institute of Technology, Cambridge, MA.

Juster, N.P. (1992) Modeling and representation of dimensions and tolerances: a survey. *Computer Aided Design*, **24**(1), 3–17.

Kumar, S. and Raman, S. (1992) Computer-aided tolerancing: the past, the present and the future. *Journal of Design and Manufacturing*, **2**, 29–41.

Lee, W.J. and Woo, T.C. (1989) Optimum selection of discrete tolerances. *Transactions of the ASME: Journal Mechanisms, Transmission, and Automaton in Design*, **111**(8), 243–251.

Lee, W.J. and Woo, T.C. (1990) Tolerances: their analysis and synthesis. *Transactions of the ASME: Journal of Engineering for Industry*, **112**, 113–121.

Lehtihet, E.A. and Dindelli, B.A. (1989) TOLCON: microcomputer-based module for simulation of tolerance. *Manufacturing Review*, **2**(3), 179–188.

Liu, S.C., Hu, S.J. and Woo, T.C. (1996) Tolerance analysis for sheet metal assemblies. *Transactions of the ASME: Journal of Mechanical Design*, **118**, 62–67.

Liu, S.C., Lee, H.W. and Hu, S.J. (1995) Variation simulation for deformable sheet metal assemblies using mechanistic models. *Transactions of NAMRI/SME*, **XXIII**, 235–240.

Luenberger, D.G. (1997) *Optimization by Vector Space Methods*, Wiley, New York, ISBN 0-471-18117-X.

Narahari, Y., Sudarsan, R., Lyons, K.W., Duffey, M.R. and Sriram, R.D. (1999) Design for Tolerance of Electro-Mechanical Assemblies: An Integrated Approach, *IEEE Transactions on Robotics and Automation*, **15**(6), pp. 1062–1079.

Nigam, S.D. and Turner, J.U. (1995) Review of statistical approaches to tolerance analysis. *Computer Aided Design*, **27**(1), pp. 6–15.

Ostwald, P.F. and Blake, M.O. (1989) Estimating cost associated with dimensional tolerance. *Manufacturing Review*, **2**(4), 277–282.

Parkinson, D.B. (1984) Tolerancing of component dimensions in CAD. *Computer Aided Design*, **16**(1), 25–32.

Parkinson, D.B. (1985) Assessment and optimization of dimensional tolerances. *Computer Aided Design*, **17**(4), 191–199.

Parkinson, A.R., Sorenson, C., Free, J. and Canfield, B. (1990) Tolerances and Robustness in Engineering Design Optimization. In *Advance in Design Automation 1990*: presented at the *1990 ASME Design Technical Conference – 16th Design Automation Conference*, Chicago, IL, DE-Vol. **23**(1), pp. 121–128.

Rong, Q., Ceglarek, D. and Shi, J. (2000) Dimensional fault diagnosis for compliant beam structure assemblies. *Transactions of the ASME: Journal of Manufacturing Science and Engineering*, **122**(4), 773–780.

Rong, Q., Shi, J. and Ceglarek, D. (2001) Adjusted least squares approach for diagnosis of compliant assemblies in the presence of ill-conditioned problems. *Transactions of the ASME: Journal of Manufacturing Science and Engineering*, **123**(3), 453–461.

Roy, U., Liu, C.R. and Woo, T.C. (1991) Review of dimensioning and tolerancing: representation and processing. *Computer Aided Design*, **23**, 466–483.

Scott, R.T. and Gabriele, G.A. (1989) Computer Aided Tolerance Analysis of Parts and Assemblies. In *Advances in Design Automation 1989*: presented at the *1989 ASME Design Technical Conferences – 15th Design Automation* Conference, DE-Vol. **19**(1), pp. 29–36. <http://www.rpi.edu/dept/mane/deptweb/faculty/member/gabriele.html>

Shalon, D., Gossard, D., Ulrich, K. and Fitzpatrick, D. (1992) Representing geometric variations in complex structural assemblies on CAD systems, in *Proceedings of the 19th Annual ASME Advances in Design Automation Conference*, American Society of Mechanical Engineers (ASME), New York, NY, **44**(2), 121–132.

Shiu, B.W., Ceglarek, D. and Shi, J. (1997) Flexible beam-based modeling of sheet metal assembly of dimensional control. *Transactions of NAMRI*, **XXV**, 49–54.

Takezawa, N. (1980) An improved method for establishing the process-wise quality standard. *Reports of Statistical Application Research, Union of Japanese Scientists, and Engineers*, **27**(3), 63–75.

Thornton, A.C. (1999) A mathematical framework for the key characteristic process. *Research in Engineering Design*, **11**, 145–157.

Voelcker, H.B. (1998) The current state of affairs in dimensional tolerancing. *Integrated Manufacturing Systems*, **9**, 205–217.

West, H.H. (1993) *Fundamentals of Structural Analysis*, New York: John Wiley and Sons, Inc.

Wu, Z., ElMaraghy, W.H. and ElMaraghy, H.A. (1988) Evaluation of cost-tolerance algorithms for design tolerance analysis and synthesis. *Manufacturing Review*, **1**, 168–179.

Zhang, H.C. (ed.) (1997) *Advanced Tolerancing Techniques*, Wiley, New York.

Biographies

Boon W. Shiu is an Assistant Professor at the Department of Mechanical Engineering at the Hong Kong Polytechnic University. He received B.Eng., M.S., and Ph.D. degrees in Mechanical Engineering in 1991, 1995, and 1996 respectively, from McGill University, and the University of Michigan. He was a senior manufacturing engineer at the General Motors Corporation for the Mid/Lux Car Group from 1996 to 1998. He performed industrial research for Chrysler, and GM for more than 6 years. Dr. Shiu's research areas include quality in manufacturing process, design in manufacturability, diagnostics for automotive assembly, and modeling in consumer products. He teaches courses on engineering design. He is a member of SME, and HKIE.

Daniel W. Apley received B.S. and M.S. degrees in Mechanical Engineering, an M.S. degree in Electrical Engineering, and a Ph.D. degree in Mechanical Engineering in 1990, 1992, 1995, and 1997, respectively, all from the University of Michigan. From 1997 to 1998 he was a postdoctoral fellow with the Department of Industrial and Operations Engineering at the University of Michigan. Since 1998, he has been with Texas A & M University, where he is currently an Assistant Professor of Industrial Engineering. His research interests include manufacturing variation reduction via statistical process monitoring, diagnosis, and automatic control and the utilization of large sets of in-process measurement data. His current work is sponsored by Ford, Solectron, Applied Materials, the National Science Foundation, and the State of Texas Advanced Technology Program. He was an AT & T Bell Laboratories Ph.D. Fellow from 1993 to 1997 and received the NSF CAREER award in 2001. He is a member of IIE, IEEE, ASME, INFORMS, and SME.

Dariusz Ceglarek is an Assistant Professor in the Department of Industrial Engineering at the University of Wisconsin, Madison. He received his diploma in Production Engineering at Warsaw University of Technology in 1987, and his Ph.D. in Mechanical Engineering at the University of Michigan in 1994. His research interests include design, control and diagnostics of multistage manufacturing processes; developing statistical methods driven by engineering models to achieve quality improvement; modeling and analysis of product/process key characteristics causality; and reconfigurable/reusable assembly systems. His current research is being sponsored by the National Science Foundation, DaimlerChrysler Corp., DCS, and the State of Wisconsin's IEDR Program. He has received a number of awards for his work including the CAREER Award from the NSF, 1998 Dell K. Allen Outstanding Young Manufacturing Engineer Award from the Society of Manufacturing Engineers (SME) and two Best Paper Awards by ASME MED and DED divisions in 2000 and 2001, respectively. He was elected as a corresponding member of CIRP and is a member of ASME, SME, NAMRI, IIE, and INFORMS.

Jianjun (Jan) Shi is an Associate Professor and the Director of the Laboratory for In-Process Quality Improvement Research (IPQI) in the Department of Industrial and Operations Engineering at the University of Michigan. He obtained his B.S. and M.S. in Electrical Engineering from the Beijing Institute of Technology in 1984 and 1987 respectively, and his Ph.D. in Mechanical Engineering from the University of Michigan in 1992. His research interests include the fusion of advanced statistical and engineering knowledge to develop IPQI methodologies that achieve automatic process monitoring, diagnosis, compensation, and their implementation in various manufacturing processes. He is a member of ASME, ASQC, IIE, and SME.

Contributed by the Manufacturing Process Planning Department